Cancer Cell
Article

# In Vivo RNAi Screen for BMI1 Targets Identifies TGF-β/BMP-ER Stress Pathways as Key Regulators of Neural- and Malignant Glioma-Stem Cell Homeostasis

Gaetano Gargiulo,[1,3] Matteo Cesaroni,[2,3] Michela Serresi,[1] Nienke de Vries,[1] Danielle Hulsman,[1] Sophia W. Bruggeman,[1] Cesare Lancini,[1] and Maarten van Lohuizen[1,*]
[1]Division of Molecular Genetics and Centre for Biomedical Genetics, The Netherlands Cancer Institute, 1066CX Amsterdam, The Netherlands
[2]The Wistar Institute, 3601 Spruce Street, Philadelphia, PA 19104, USA
[3]These authors contributed equally to this work
*Correspondence: m.v.lohuizen@nki.nl
http://dx.doi.org/10.1016/j.ccr.2013.03.030

## SUMMARY

**In mouse and human neural progenitor and glioblastoma "stem-like" cells, we identified key targets of the Polycomb-group protein BMI1 by combining ChIP-seq with in vivo RNAi screening. We discovered that *Bmi1* is important in the cellular response to the transforming growth factor-β/bone morphogenetic protein (TGF-β/BMP) and endoplasmic reticulum (ER) stress pathways, in part converging on the *Atf3* transcriptional repressor. We show that *Atf3* is a tumor-suppressor gene inactivated in human glioblastoma multiforme together with *Cbx7* and a few other candidates. Acting downstream of the ER stress and BMP pathways, ATF3 binds to cell-type-specific accessible chromatin preloaded with AP1 and participates in the inhibition of critical oncogenic networks. Our data support the feasibility of combining ChIP-seq and RNAi screens in solid tumors and highlight multiple $p16^{INK4a}$/$p19^{ARF}$-independent functions for *Bmi1* in development and cancer.**

## INTRODUCTION

Glioblastoma multiforme (GBM) is the most common primary malignant brain tumor with a dismal prognosis despite multimodal therapies (Park et al., 2010). The systematic investigation of critical cancer genes in genetically matched mouse models has been enhanced by the recent molecular classification of human GBM in molecular subtypes and by the launch of RNAi screens in vivo (Bric et al., 2009; Meacham et al., 2009; Verhaak et al., 2010). However, in vivo RNAi screening for solid tumors requires the rational selection of limited targets to overcome practical limitations in transplantation assays and potential off-target effects.

The polycomb (PcG) repressive complex 1 (PRC1) is required for adult stem cell functions and its activity is hijacked by cancer cells to silence tumor suppressive mechanisms (Sparmann and van Lohuizen, 2006).

Ablation of PRC1 member *Bmi1* strongly affects the number of normal neural stem cells (NSCs) in adult mice and delays gliomagenesis, highlighting a critical role for *Bmi1* in normal and aberrant self-renewal. *Bmi1* activity in NSCs relies in part on the repression of the Cdkn2a locus (encoding for $p16^{INK4a}$ and $p19^{ARF}$), whereas additional functions in adult brain and glioma homeostasis remain largely unknown (Molofsky et al., 2003; Bruggeman et al., 2007). *Bmi1* depletion in primary mouse and human glioma-initiating cells (GICs) resulted in less aggressive tumors and cancer cell apoptosis, respectively, which are accompanied by a substantial transcriptome reprogramming underscoring the importance of functionally characterizing the BMI1 target genes and their pathways implicated in NSC

### Significance

Malignant gliomas are incurable brain tumors in which major tumor-suppressor genes are genetically inactivated. In these tumors, the Polycomb protein *Bmi1* plays an oncogenic role, so far poorly understood. By combining ChIP-seq for BMI1 and in vivo RNAi screens in a mouse model for glioma, we identified tumor-suppressor genes whose expression can be potentially restored by dedicated pharmacological strategies. Our results illustrate that validated oncogenes can be mechanistically dissected by rational designing of shRNA screening in vivo. Broadly, *Bmi1* appears to endorse self-renewal by integrating a plethora of signaling cues into defined transcriptional outputs. Furthermore, *Atf3* and *Cbx7* are important modulators downstream of *Bmi1* oncogenic activity in gliomas, extending the previous observation that *Bmi1* mediates important $p16^{INK4a}$/$p19^{ARF}$-independent functions.

maintenance and gliomagenesis (Bruggeman et al., 2007; Abdouh et al., 2009; Facchino et al., 2010).

Transforming growth factor (TGF)-β and bone morphogenetic protein (BMP) signaling are important in NSC and brain tumor cell homeostasis (Watabe and Miyazono, 2009). TGF-β supports glioma cell proliferation, migration, and survival and affects immunosurveillance (Seoane, 2009; Anido et al., 2010). BMP signaling promotes the differentiation of embryonic neural progenitor cells and, likewise, deprives glioblastoma stem-like cells (GSCs) of self-renewal capacity by inducing astrocytic commitment, in turn reducing glioma growth and associated mortality (Lim et al., 2000; Chirasani et al., 2010). TGF-β/BMP downstream target *Id1* is highly expressed in neural and glioma stem cells, where it contributes to self-renewal. *Id1* expression is directly repressed by the stress-responsive ATF3 transcription factor activated in a negative feed-forward loop upon TGF-β stimulation in epithelial cells but not in GSCs (Kang et al., 2003; Anido et al., 2010), suggesting a glioma-specific inactivation of the stress-response pathway. The PcG pathway affects GSCs response to BMP2 signaling due to cancer-specific silencing of its receptor (Lee et al., 2008), but the extent and the implications of the interplay between PcG, TGF-β/BMP, and stress-response pathways are not yet fully understood.

In this study, we combined ChIP-seq and in vivo RNAi screenings to investigate the mechanisms underlying *Bmi1* functions in neural progenitor cells (NPCs), GICs, and GSCs.

## RESULTS

### BMI1 Target Genes Are Regulated during Neural Stem Cell Lineage Commitment and Deregulated in *Bmi1* Knockout Brain

To determine the comprehensive BMI1 transcriptional network in neural progenitor and brain tumor cells, we applied an ad hoc ChIP-seq strategy to early-passage NPCs, astrocytes, and glioma-initiating cells (GICs; see Supplemental Experimental Procedures and Table S1 available online). Senescence-impaired subventricular zone (SVZ) NPCs are endowed with an extended lifespan but similar developmental potential (Molofsky et al., 2006) and are highly tumorigenic in vivo when transduced with the glioma-specific *EgfrvIII*, except when combined with *Bmi1* deletion that impairs their malignancy (Bruggeman et al., 2007). Importantly, *EgfrvIII*;*Cdkn2a*$^{-/-}$ GICs closely mirror the human "classical" GBM (Verhaak et al., 2010).

In NPCs, BMI1 binding preferentially occurred at DNA elements largely overlapping with protein-coding genes. Strikingly, despite a cell-type-specific expression fingerprint, the vast majority of the BMI1 network of protein-coding and noncoding genes appears to be independent of developmental stage and tumorigenic potential (Figures 1A and S1A–S1D; data not shown).

ChIP-qPCR in *Bmi1*$^{-/-}$ and wild-type NPCs confirmed the high sensitivity and specificity of our procedure (Figures 1B and 1C). Also, we found that *Bmi1* is important to maintain H3K27me3 levels at binding sites (Figure S1E).

BMI1 binding globally correlates with low gene expression levels in NPCs, while several target genes are differentially expressed and linked in molecular networks in NPCs progeny, such as astrocytes, oligodendrocytes, and neurons. Astrocyte-specific targets showed significantly lower expression in glial cells than in postnatal neurons or oligodendrocytes, underscoring the specificity of this analysis (Figure 1D and S1F–S1I). To a large extent, BMI1 represses neuronal lineage-specific genes in line with the astrocytic origin of SVZ-NPCs (Kriegstein and Alvarez-Buylla, 2009). Finally, several BMI1 target genes showed a remarkable transcriptional deregulation in brain cancers, including GBM and medulloblastoma (Figures S1L and S1M), in agreement with *Bmi1* function to be important in these tumors (Leung et al., 2004; Bruggeman et al., 2007).

To understand the consequences of *Bmi1* ablation on target gene expression, we performed global RNA-seq profiling of NPCs propagated under growth factor defined conditions and infected with doxycycline (dox)-inducible RNAi (BMI1 and GFP) constructs, as well as of adult brain tissue. Only 4.8% (61/1,270) of the neural BMI1 target genes systematically require *Bmi1* for continuous repression, such as the well-known PcG targets *Hox* genes (Figure 1E), whereas *Bmi1* loss had a greater effect on the adult brain, with ~500 genes upregulated exclusively in the *Bmi1*$^{-/-}$ mouse brain (Figures 1F and 1G).

Importantly, several key developmental regulators are BMI1 targets (Figure S1F) and some of these were found significantly upregulated in *Bmi1*$^{-/-}$ brain tissues, including *Tal1, Runx3, Pitx2*, and *Foxf1*, as well as long noncoding RNAs (e.g., *Igf2as* and *Foxl2os*; Figure 1G). Because of their direct functions in neural lineage commitment and of related pathways such as Notch, TGF-β/BMP and Wnt, deregulation of such BMI1 targets is predicted to have widespread effects in neural development beyond just affecting cell cycle control (Kioussi et al., 2002). This may explain the incomplete rescue of *Bmi1* developmental defects by the sole codeletion of *Cdkn2a* (e.g., reduced brain size and cerebellar foliation; van der Lugt et al., 1994; Bruggeman et al., 2005).

Collectively, our data show that BMI1 binds to protein-coding and noncoding genes critical for neural lineage commitment and, possibly, relevant for brain cancers.

### Bmi1 Binds to Genes Involved in TGF-β and BMP Signaling in Normal and Tumor Cells

To understand if BMI1 target genes are interconnected into specific signaling cascades, we performed ingenuity pathway analysis (IPA).

Reasoning that mouse-human conserved BMI1 target genes would be more informative in this analysis, we performed additional Bmi1 ChIP-seq profiling of primary human fetal NPCs (Sun et al., 2009) and GSCs (Pollard et al., 2009). GBM1 and GBM5 GSC lines were previously characterized for developmental potential and tumorigeneicity and we further classified them as "mesenchymal" and "proneural" GBM, respectively, using gene set enrichment analysis (GSEA) and qPCR (Figure S2A; data not shown). Hence, our BMI1 profiles cover the three best-characterized GBM subtypes.

Next, we analyzed pathways enriched in target genes common to all our BMI1 profiles, unraveling a core network of PcG target genes associated with TGF-β and BMP signaling pathways (Figures 2A and 2B). Moreover, these pathways featured the highest significance in mouse-human NPCs BMI1 target genes and among genes upregulated in *Bmi1*$^{-/-}$ mouse brain (Table S2; data not shown).

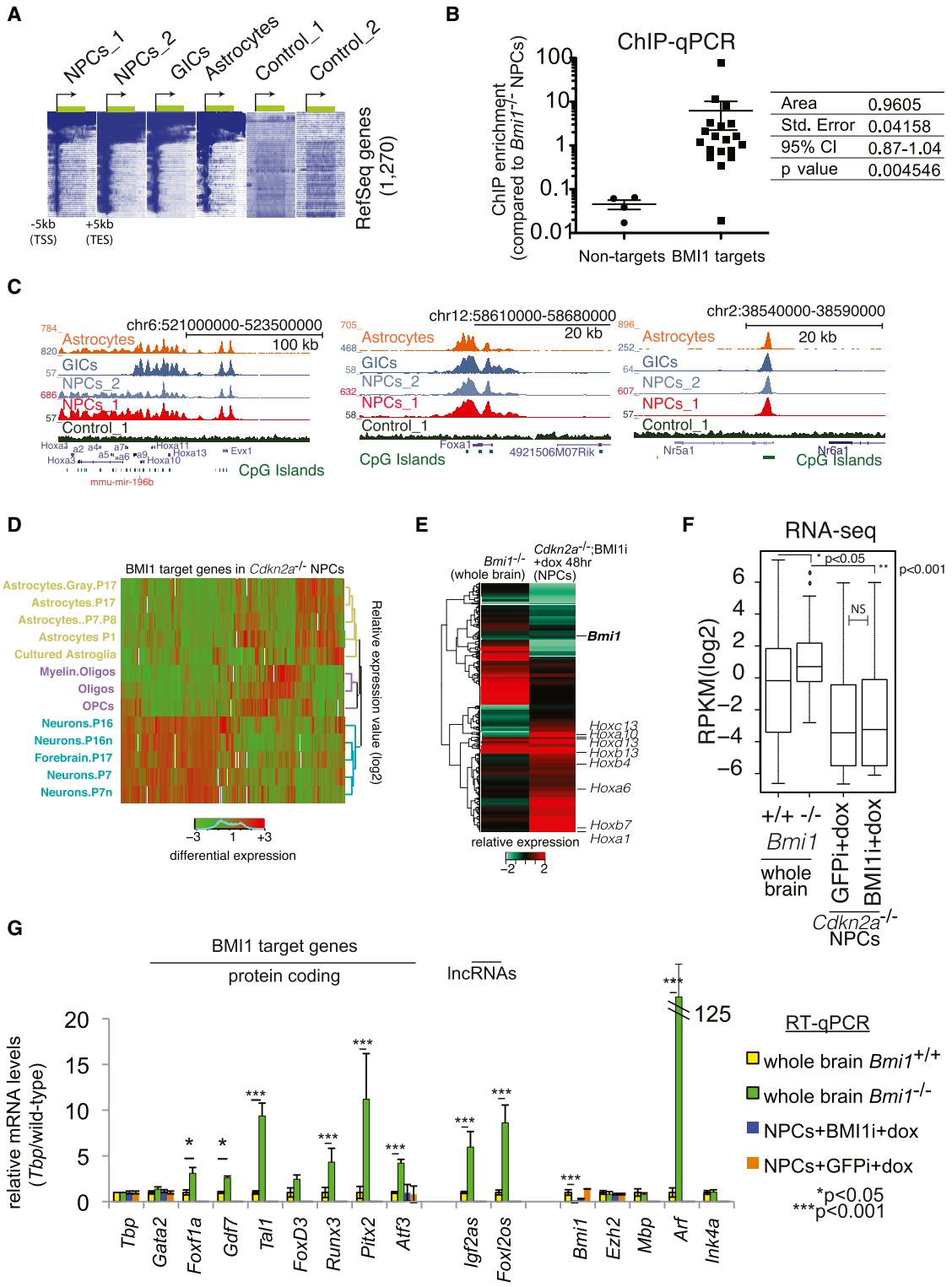


**Figure 1. Genome-wide BMI1 Target Genes and Their Expression Changes in Normal and *Bmi1*-Depleted NPCs and Mouse Brains**

(A) Horizontal lines represent individual genes and dark blue high reads count. Input DNA control depicts random distribution. Supplemental experimental procedures include detailed description of cells and bioinformatics. TSS and TES are transcription start and end sites.

(B) ROC plot of ChIP-qPCR validation of BMI1 peaks in NPCs. Results were expressed as enrichment over *Bmi1* deficient NPCs (error bar = mean ± SEM; n = 2).

(C) UCSC genome browser view of ChIP-seq profiles for the indicated cells.

(D) BMI1 target genes expression in murine brain cells (Cahoy et al., 2008). P, postnatal; OPCs, oligodendrocyte progenitor cells; Gray, gray matter; cultured astroglia, astrocyte-enriched tissue-cultured cell.

*(legend continued on next page)*

TGF-β and BMP receptors signal through a complex cascade of intracellular events including phosphorylation of SMAD2 (TGF-β) or SMAD1-5-8 (BMPs) ultimately leading to nuclear translocation of SMAD4 and target gene regulation. A prominent role for BMP cytokines during neural development has been substantially demonstrated (Kriegstein and Alvarez-Buylla, 2009). To determine whether *Bmi1* is important to coordinate a transcriptional response to BMP signaling, we performed RNA-seq in NPCs after dox-induced depletion of *Bmi1* and exposure to BMP4. Strikingly, even after a short-term and low-dose treatment, BMI1 target genes showed preferential upregulation in *Bmi1*-depleted cells (Figure 2C). RT-qPCR confirmed BMI1/BMP4 targets to be more strongly upregulated in *Bmi1*-depleted progenitors (Figures S2B and S2C).

Because BMP4 signaling is known to induce the differentiation of embryonic neural progenitor cells into astrocytes (Lim et al., 2000), we extended our RNA-seq profiles to NPCs treated with fetal bovine serum (routinely used to differentiate NPCs), including low and high concentrations (1%–10%) at different time points. Unsupervised clustering based on BMI1 target gene expression demonstrated that NPCs differentially respond to signaling cues when *Bmi1* level is artificially reduced (Figure 2D), indicative of a broadly altered response to differentiation stimuli.

To understand the significance of this altered response, we next assayed the proliferative and differentiation response of *Bmi1*;*Cdkn2a*$^{-/-}$ NPCs to morphogens. While TGF-β1 and TGF-β2 did not significantly alter *Bmi1*;*Cdkn2a*$^{-/-}$ NPCs growth on laminin-coated dishes or Nestin and GFAP expression, BMP4-treated NPCs significantly arrested when compared to *Cdkn2a*$^{-/-}$ NPCs, and their self-renewal was more drastically compromised (Figures 2E and 2F; data not shown). This altered response was accompanied by lower induction of the TGF-β/BMP target *Id1* and by unscheduled expression of its inhibitor Atf3 (Figures 2G, S2D, and S2E; Kang et al., 2003). *Atf3* derepression occurred also in *Bmi1* knockdown BMP4-treated NPCs, underscoring a critical role of *Bmi1* dose in regulating *Atf3* levels (Figure S2E).

Next to the known role for *Id1* in primitive NSCs self-renewal (Nam and Benezra, 2009), we provide evidence in adult NPCs that *Bmi1* cooperates with critical extracellular stimuli such as BMPs in regulating tissue homeostasis, by fine-tuning the expression of direct effectors or inhibitors of this pathway, as exemplified by *Id1-Atf3*.

## Conserved BMI1 Target Genes in Glioma Include Tumor-Suppressor Genes

We reasoned that use of in vivo RNAi to ablate BMI1 target gene function would help select out cancer genes relevant for glioma.

First, we verified that *Bmi1* expression is not restricted to specific GBM subtypes. We found evidence for *Bmi1* expression in the vast majority of patients with GBM (>89%), regardless of the molecular subtype classification, and its expression correlates with average patient survival. Finally, immunohistochemical analysis of high-grade glioma tissue microarrays using NKX2.2 and TRADD as proneural and mesenchymal markers, respectively, demonstrated BMI1 expression to be independent of GBM subtype markers (Figures S3A–S3C; data not shown).

Next, we generated an shRNA library of conserved BMI1 target genes in glioma (hereafter referred to as CBTG library) by using cross-species conservation (Figure 3A; Table S3). The CBTG library included all of the 129 BMI1 targets for which three to six shRNAs were available (Broad Institute TRC1 library), several PcG genes, and ten shRNAs against epidermal growth factor receptor (EGFR) as controls. This resulted in a pool of 789 hairpins, each represented ~130-fold when 100,000 cells are injected per animal. In bulk, seven animals ensure ~1,000× representation of this library.

Loss of *Cdkn2a* and gain of *EgfrvIII* are sufficient to initiate gliomagenesis in mouse models (Holland et al., 1998; Bachoo et al., 2002), and we have previously demonstrated the homogeneous and potent grafting efficiency of such GICs and that loss of *Bmi1* does not reduce the number of tumor-initiating cells (Bruggeman et al., 2007). These features suggest that our model is well suited to accommodate a complex library of shRNAs.

To test whether our CBTG library contains tumor-promoting shRNAs, which are predicted to increase tumorigenic potential of our GICs, we set out a competition assay in vivo (Figure 3B). Because *Bmi1* expression in GICs could restrict target gene expression, we reasoned that its in vivo depletion would increase our ability to identify critical target genes. To this end, we used the dox-responsive shBMI1 (BMI1i) and shGFP (GFPi), and verified their ability to ablate protein expression in mouse tumors (Figure 3C). Both GFPi- and BMI1i-CBTG tumors showed similar histopathologic features of high-grade gliomas and survival kinetics regardless of *Bmi1* ablation (Figures S3D and S3E).

CBTG-modified cells were injected into recipient animals with a ratio of 1 to 10 or 1 to 100 with non-CBTG-modified GICs, and tumor formation was monitored by noninvasive bioluminescence. After 7–9 weeks, all of the animals showed luciferase emission, except for non-CBTG controls (Figures 3D and 3E). Furthermore, when glioma "stem-like" cell lines were derived from three random tumors generated using as little as 1/100th CBTG-modified GICs, only these cells contributed to tumor-propagating lines (CBTG-modified cells were retrospectively identified by fluorescence-activated cell sorting [FACS] because they contain a dox-inducible shRNA against GFP; Figure 3F). Single sphere analyses revealed that multiple shRNAs integrations are infrequent events in our setting (Figure S3F).

Together, our data suggest that CBTG-modified cells within a mixed tumor are endowed with a higher ability to initiate and

(E) Heatmap representation of RNA-seq profile of *Bmi1*$^{-/-}$ whole brain, littermate controls, and of doxycycline-treated NPC bearing a lentivirus expressing *Bmi1* or GFP shRNAs under a dox-responsive promoter. Common deregulated BMI1 targets normalized by controls are shown, FC > 1.5, $p < 0.02$ (Student's t test; n = 2).

(F) Log2 fold changes in transcript level of BMI1 target genes de-regulated in the *Bmi1*$^{-/-}$ murine brains. Note that significant upregulation occurs only in vivo (Student's t test; n = 2).

(G) RNA-seq profile validation by RT-qPCR. Selected significant comparisons are shown (two-way ANOVA).

Error bars = ± SD. See also Figure S1 and Table S1.

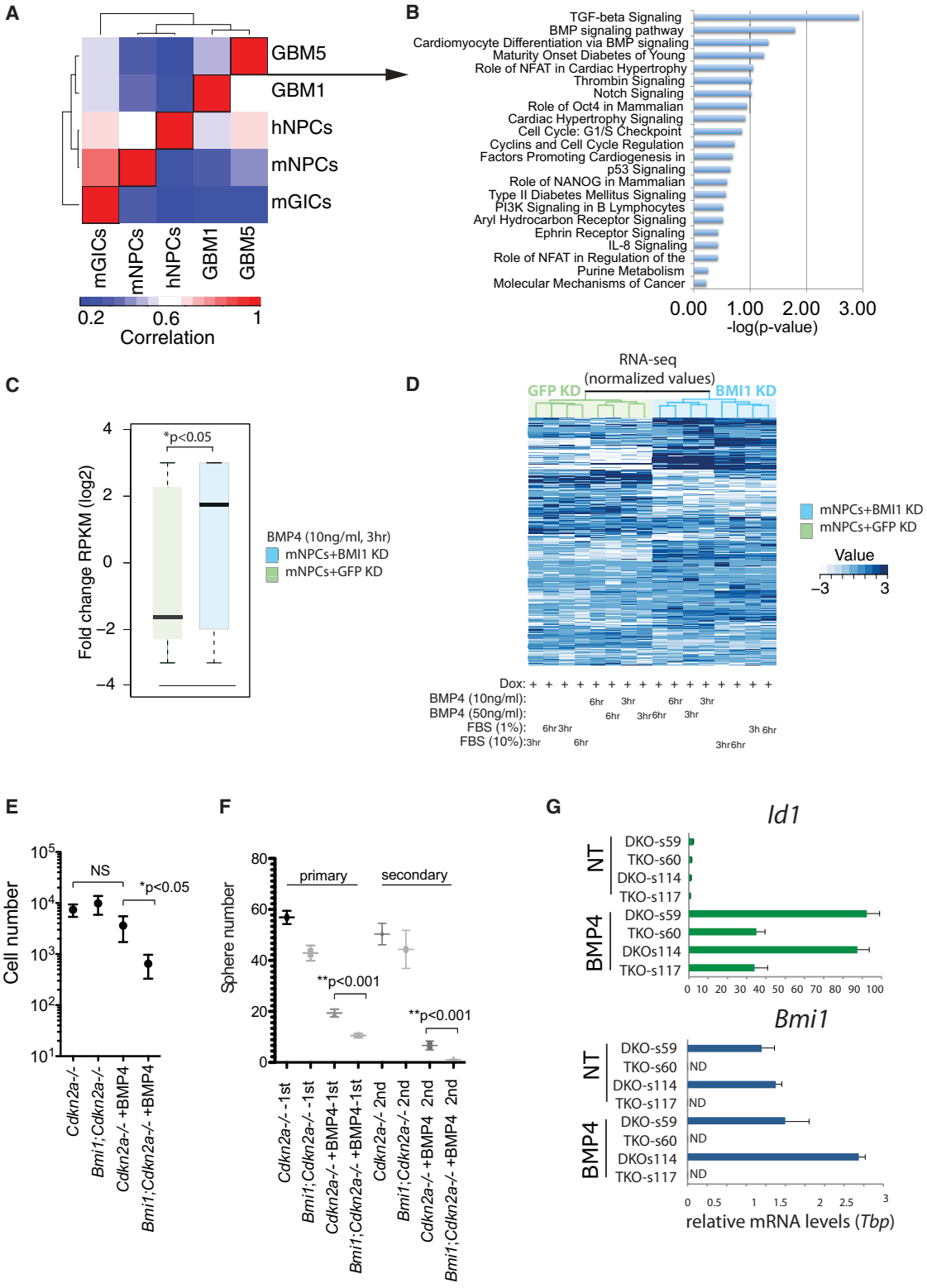


**Figure 2. *Bmi1* Is Important to Coordinate an Appropriate Transcriptional Response to TGF-β/BMP Signaling**

(A) Two-by-two correlation of each ChIP-seq profiles to each other. Rows and columns (peaks) are sorted based on Spearman's rank-order. Red and blue represent high and low correlations, respectively.

(B) Ingenuity pathway analysis of mouse-human conserved BMI1 targets in NPCs and GBM "stem-like" cells from (A).

(C) RNA-seq profile of BMI1 targets in *Bmi1*-depleted NPCs upon short-exposure to BMP4 (3 hr; 10 ng/ml; FC > 0.5; Student's t test).

*(legend continued on next page)*

propagate the disease, indicating the presence of tumor-promoting shRNAs in the CBTG library.

### A Forward In Vivo Genetic Screen for Epigenetically Silenced Tumor-Suppressor Genes in Glioblastoma

To uncover the identity of tumor-promoting shRNAs within all CBTG tumors, we used HT-sequencing of glioma-enriched shRNAs.

Tumor-enriched shRNAs correspond to tumor suppressor genes (TSGs), whereas hairpins targeting oncogenes are depleted during tumor grafting (Bric et al., 2009; Meacham et al., 2009). Our screening relies on the orthotopic transplantation of GICs transduced with dox-responsive shRNAs targeting *Bmi1* (or GFP as control) and with a pool of puromycin-selectable shRNAs directed against BMI1 target genes (CBTG library). Reads obtained by sequencing tumor-derived hairpins are normalized by the hairpins retrieved in the control cells (i.e., before injection). In parallel, CBTG-modified GICs are propagated in vitro for over six passages (~3 weeks) to trace single hairpin segregation under optimal growth conditions (Figure 4A).

Previous studies have shown that 26%–40% of the initial library complexity could be maintained in myc-driven lymphomagenesis (Meacham et al., 2009). In a pilot experiment comprising seven tumors (i.e. ~1,000× the CBTG library), we noted a median complexity of 31% (16%–88%) independent of the initial library complexity, which was retained in vitro (Figures 4B and 4C). By subsequent rounds of sequencing, we excluded that in vivo dropout is strongly dependent on suboptimal saturation (data not shown). Because each hairpin within our library theoretically had ~130-fold representation per mouse, loss of shRNAs during gliomagenesis may be explained by either random tumor clone outgrowth, or by functional depletion of tumor-essential (or neutral) shRNAs.

To discriminate between these two possibilities, we first analyzed the distribution of control shRNAs targeting EGFR, which is required for efficient gliomagenesis. Significant depletion of shRNAs targeted EGFR in mouse tumors, but not in vitro. We demonstrated strong in vivo functional selection confirming the feasibility of the screen (Figures 4D and S4A). As an exception, one shRNA targeting simultaneously endogenous EGFR and EGFRIII was reduced in vitro as well. EGFR immunostaining confirmed protein expression in mouse gliomas (Figure S3F).

Next, we performed the entire procedure de novo, reasoning that if shRNAs segregation in vivo entails a functional selection, enrichments should be reproducible. Hypergeometric distribution is indicative of a significant overlap between the two experiments, after selection of hairpins whose enrichment was found in three to five or more animals per experiment (Figure 4E; Table S3; data not shown). Combining both experiments, we reached a final number of 20 tumors, nine of which were generated in the presence of continuous suppression of *Bmi1* expression. After normalization on input cells, heatmap correlation between in vitro and in vivo shRNA-seq showed that loss of *Bmi1* is—to some extent—neutral to the final pattern of shRNAs enriched in vivo, and more importantly, that gliomagenesis promotes a specific set of tumor-enriched shRNAs, underscoring the significance of this in vivo screen (Figure 4F; Table S3).

To identify candidate tumor-suppressor genes epigenetically silenced in human GBM, yet limiting the contribution of "passenger shRNAs" (i.e., enriched by either off-target or non-cell autonomous effects), we used several qualitative indicators. First, we selected genes when at least two independent shRNAs were present and enriched in both experiments ($n = 106$, $p < 7.8 \times 10^{-81}$). Next, we searched for evidence of more than one copy of the corresponding human loci in GBM, and for DNA methylation (Figure 4F). In fact, DNA hypermethylation and PcG binding have been previously shown to overlap in human tumors (Ohm et al., 2007; Schlesinger et al., 2007; Widschwendter et al., 2007). Alternatively, pathway analysis can help identify relevant candidates (Figures S4B–S4E). Notably, the vast majority of glioma-enriched shRNA-targeted genes are expressed in adult brain tissue and implicated in neural development, indicating that preventing differentiation likely is a general feature promoting gliomagenesis.

While genes not methylated in GBM yet passing the other filters could still have tumor-suppressive functions, we focused on six candidate tumor-suppressor genes that are potentially restorable in human glioma (Figures 4F and S4E). *Alx3* was previously indicated as an hypermethylated tumor-suppressor gene in neuroblastoma and *Ptprd* was validated as a TSG in GBM (Wimmer et al., 2002; Veeriah et al., 2009). Importantly, DNA methyltransferase inhibitor 5-azacytidine alleviates repression for these genes and even more effectively in combination with dox-induced *Bmi1* inhibition (Figure 4G).

Conversely, when we interrogated shRNAs significantly depleted in vivo, and with specific criteria as in Figure S4F, we identified candidate oncogenes that could be relevant for the classical GBM subtype, including validated oncogenes in GBM such as *Ccnd2*, and *Klf6* (Büschges et al., 1999; Kimmelman et al., 2004). Overall, our data support the feasibility of a forward genetic screen in solid tumors.

### Suppression of *Atf3* and *Cbx7* in *Bmi1*-Depleted Glioma-Initiating Cells Accelerates Tumorigenesis and Impairs Animal Survival

Next, we selected out *Atf3* and *Cbx7* as candidate TSGs in glioma because they showed dichotomous and context-dependent functions in diverse tumor models and were not implicated in glioblastoma (Scott et al., 2007; Thompson et al., 2009; Forzati et al., 2012).

(D) BMI1 targets expression for NPCs treated with BMP4 or FBS as indicated. Heatmap represent RNA-seq data as normalized over dox-treated GFPi NPCs controls (n = 2).
(E and F) *Cdkn2a*$^{-/-}$ and *Bmi1*$^{-/-}$;*Cdkn2a*$^{-/-}$ NPCs were cultured as adherent monolayer (E) or neurospheres (F) in the presence of EGF/FGF2 ± BMP4. Selected comparisons are shown (1-way ANOVA). Note that *Bmi1*-depleted NPCs are more sensitive to BMP4 cytostatic and differentiation activity.
(G) RT-qPCR of two adherent NPCs lines treated with BMP4. Results were normalized on the ubiquitous gene. DKO = *Cdkn2a*$^{-/-}$; TKO = *Bmi1*$^{-/-}$; *Cdkn2a*$^{-/-}$; ND = non-detected.
Error bars = ± SD. See also Figure S2 and Table S2.

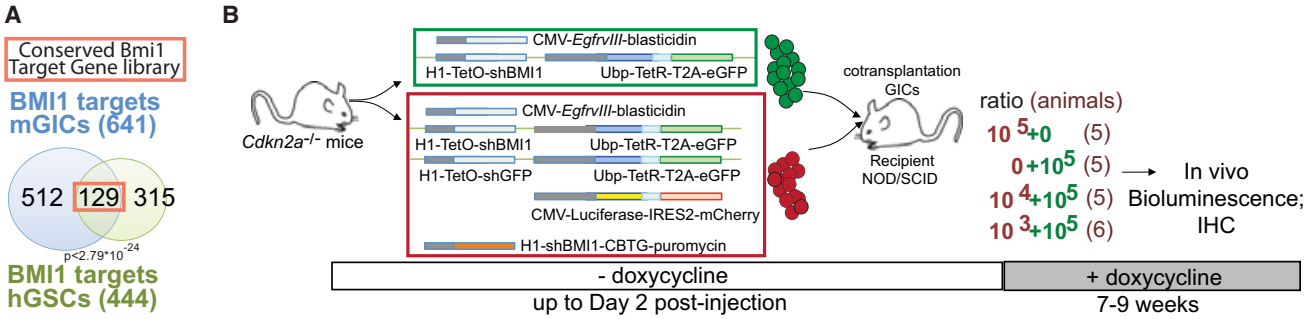


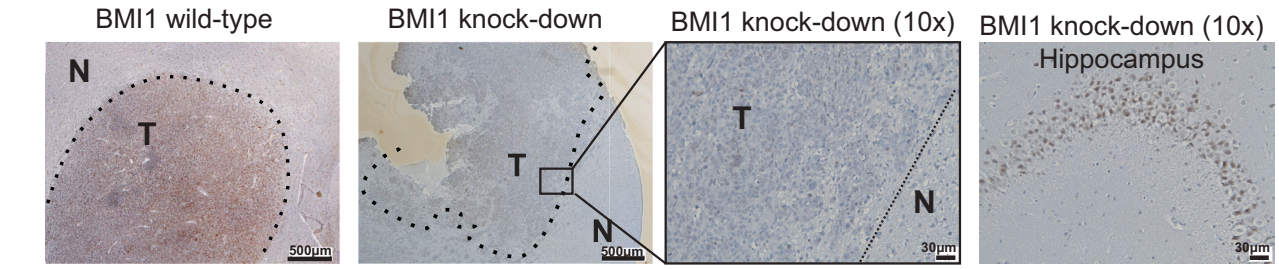


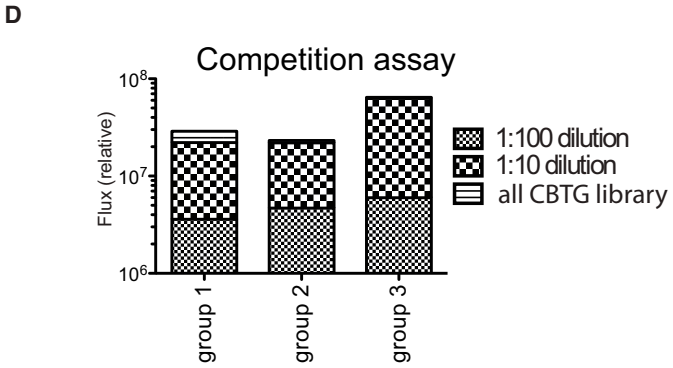


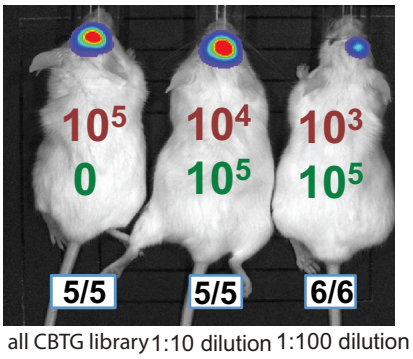


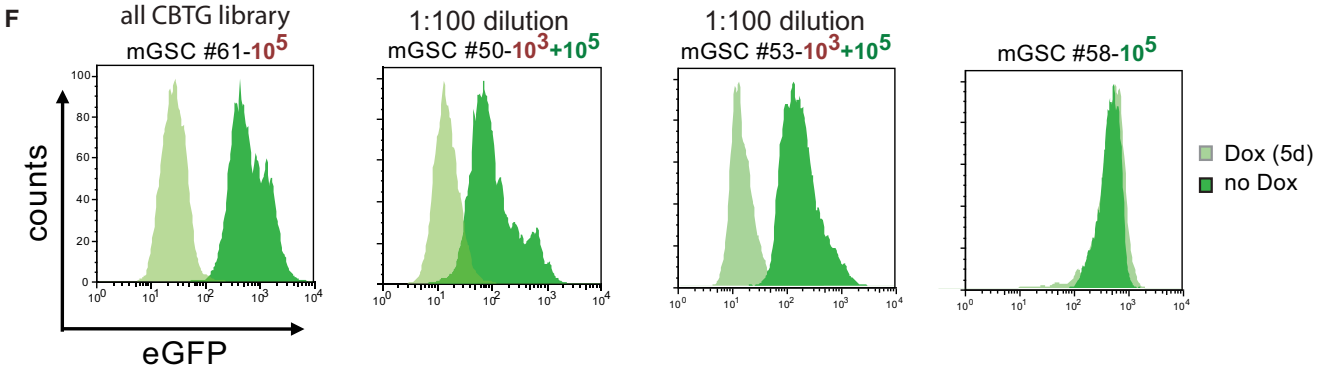


(legend on next page)

To confirm their putative role as TSGs in glioma, we introduced two single hairpins targeting either *Atf3* or *Cbx7* in GICs, followed by intracranial transplantation. *Egfrv*III*;Cdkn2a*$^{-/-}$;BMI1i cells bearing two independent shRNAs per gene showed enhanced tumorigenic potential, dramatically lowering animal survival to < 3 weeks after transplantation (Figure 5A). As expected, GICs induced large hypercellular neoplastic lesions with defined margins but local invasion. Mitoses were readily seen, and, more rarely, these tumors also showed large-sized anaplastic and multinucleated giant cells, all features of grade IV World Health Organization classification. However, only *Atf3*- and *Cbx7*-depleted tumors comprehensively showed all the features of human GBM such as multifocal necrosis, fibrovascular stroma, non-neural cells such as osteoclasts, and hemorrhages (Figures 5B–5E, S5A, and S5B). Notably, all these features were more often associated with *Atf3* loss, indicating an inverse correlation with animal survival. ATF3 immunostaining was often seen in control tumors, with increased nuclear localization surrounding apoptotic cells and was markedly reduced in *Atf3*-depleted tumors (Figure 5D). RT-qPCR and western blotting confirmed *Atf3* knockdown (Figure S5C).

These shRNAs efficiently knockdown their targets while not affecting tumor-sphere formation, and in vitro puromycin selection prevented cells devoid of the desired shRNAs to affect the in vivo growth (Figures S5D and S5E).

To further exclude that in vivo enrichments would result from pre-existing in vitro defects, we cloned six shRNAs targeting *Atf3* (2 shRNAs), *Cbx7*, *Prdm1*, *Lmx1a*, and *Hand1* in dox-inducible RNAi vectors and found that knockdown did not affect multipotency or differentiation, as gauged by sphere formation ability and SOX2/GFAP FACS staining (Figure S5F).

Thus, underscoring the value of combined ChIP-seq/RNAi screen for BMI1 target genes implicated in glioma, we validated *Atf3* and *Cbx7* as TSGs in the context of the in vivo tumor microenvironment.

## ATF3 Nuclear Localization Is Excluded from High-Grade Astrocytomas

To investigate ATF3 in human brain tumors, we performed tissue array analysis to compare ATF3 protein levels between 63 low- and high-grade astrocytoma/glioma and eight normal brain tissue samples.

We found that only 38% (24/63) of the tumors showed patches of nuclear staining for ATF3, and 80% of these (19/24) were low grade (Figures 6A and 6B). The remaining immunoreactive samples, including normal brain tissues, showed a cytoplasmic staining. This feature was also seen in high-grade mouse lesions (Figure 5D; data not shown).

Being a transcription factor, our data suggest that ATF3 regulation in glioma may involve at least two layers: gene expression and subcellular localization. ATF3 more often localized to the nucleus of low-grade astrocytomas, but was either absent or excluded from the nucleus in all the GBM samples, compatible with an impaired function in high-grade tumors. In fact, evaluation of data contained in the REMBRANDT database (molecular repository for brain cancers) showed that patients with "intermediate" levels of *Atf3* had a moderate but statistically significant extended lifespan than patients with "downregulated" expression (Figure 6C). This analysis was based on patients with potential nuclear localization of ATF3, that is, those with astrocytoma but not GBM. Age at diagnosis did not alter survival of patients with downregulation of *Atf3*, because median age for this group is in fact lower (median = 40–44 versus 50–54 years).

Even though in human gliomas *Atf3* expression is generally low, we found a moderately significant inverse correlation with *Bmi1* expression ($p = 0.026$; Figure S6A and S6B). Likewise, patients with medulloblastoma (MD) and *Atf3*$^{high}$-*Bmi1*$^{low}$ gene expression levels had better survival times (data not shown). Costaining for BMI1 and ATF3 in the glioma tissue array, however, indicated that BMI1 does not prevent ATF3 expression at single cell level (Figure S6C), perhaps suggesting that BMI1 regulation may affect ATF3 levels rather than on-off switching. Nonetheless, in cells co-expressing BMI1 and ATF3, the latter was most often cytoplasmic, and as such transcriptionally inactive.

Of note, *Cbx7* expression showed similar correlation with survival time for patients with glioma (Figure S6D).

Based on the retrospective nature of these analyses, we conclude that BMI1 target gene *Atf3* holds prognostic significance for human brain tumors.

## BMP Signaling and ER Stress-Activated ATF3 Engages Open Chromatin Preloaded with AP1 Transcription Factor

The brain microenvironment impairs gliomagenesis because endogenous NPCs can release BMP7 and endovanilloids, leading to differentiation and ER stress-dependent apoptosis, respectively(Chirasani et al., 2010; Stock et al., 2012). Because

**Figure 3. BMI1 Target Genes RNAi Promotes Growth Advantage In Vivo**

(A) A conserved BMI1 target gene (CBTG) library is assembled pooling multiple shRNAs per gene, targeting mouse (GICs and GL261) and human (GBM1 and GBM5) BMI1 target genes. Additional hairpins include ten control shRNAs targeting EGFR receptor and other PcG genes.

(B) In vivo competition assay to assess the tumorigenic potential of $10^3$ or $10^4$ cells CBTG library-luciferase bearing cells (10× and 1× library representation) co-injected with $10^5$ GICs. Transduced constructs are indicated.

(C) Validation of *Bmi1* ablation in vivo. NOD/SCID mice intracranially injected with GICs carrying a dox-responsive shGFP (GFPi) or shBMI1 (BMI1i) received 20 μg/ml Dox and 0.01% sucrose drinking water from day 2 postinjection. Representative BMI1 IHC of a GFPi or BMI1i tumors. Inset shows higher magnification of *Bmi1* KD glioma IHC. Normal brain BMI1 staining is shown as control. T, tumor; N, normal.

(D) 1,000 CBTG-modified cells can contribute to tumorigenesis. Noninvasive bioluminescence performed on animals bearing tumors composed of CBTG-luciferase- and nonmodified cells (no luciferase), in excess of 10-fold or 100-fold. Note the 100-fold diluted shRNA modified cells high luciferase signal (Flux).

(E) A representative set of animals from (D) is shown (group 1).

(F) FACS analysis of two representative GSC lines established from tumors initiated with 100-fold excess of nonmodified cells. Loss of GFP signal upon dox treatment (see B) confirms that these cells derive from CBTG-modified cells. Note that all CBTG-modified and 100× dilution-derived GSCs lines FACS profiles are indistinguishable.

See also Figure S3.

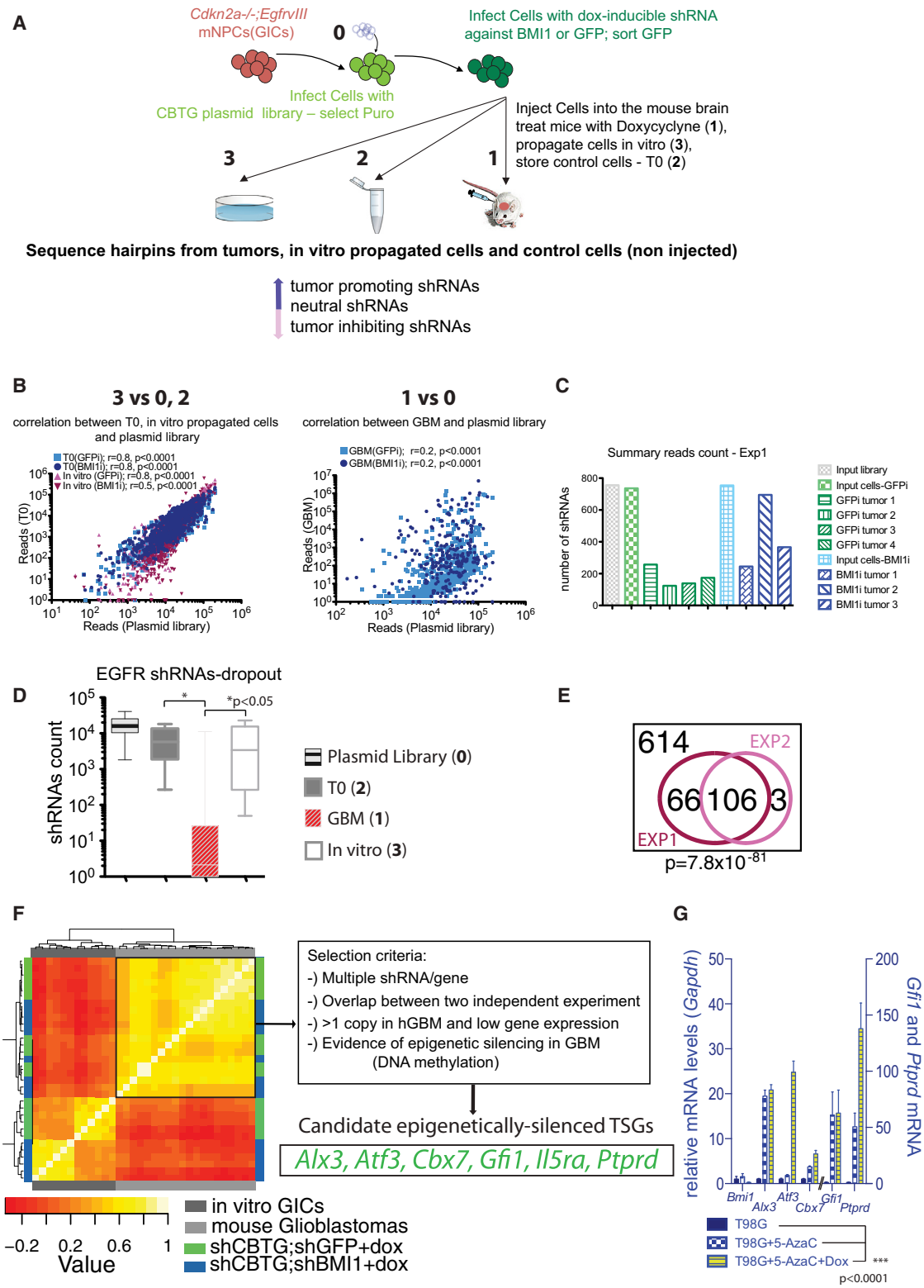


**Figure 4. A Forward Genetic Screen to Identify Epigenetically-Silenced Tumor Suppressors in GBM**

(A) RNAi in vivo experiment outline.

(B) Scatter plot correlation of plasmid library shRNA reads and transduced/selected GICs before transplantation (T0) or propagated in vitro under stem cell conditions (left). The right plot illustrates correlation for GFPi or BMI1i tumor; r, Pearson correlation coefficient.

(C) The number of unique hairpins present in the plasmid library, T0 cells, and tumors from a first experiment comprising four GFPi and three BMI1i CBTG tumors (5–7 weeks of in vivo selections).

*(legend continued on next page)*

this response is active in all transplantation-based studies (including our in vivo RNAi screen) and *Atf3* has been functionally implicated in this signaling cascade, we investigated whether BMP7 and the synthetic vanilloid arvanil would affect GICs growth in soft agar. Indeed, arvanil totally abrogated colony formation and neither epidermal growth factor (EGF)/basic fibroblast growth factor (bFGF) nor TGF-β1 could rescue this inhibitory effect, neither did the sole *Atf3* overexpression or knockdown significantly affect GIC growth in a bulk tumorsphere assay, underscoring the importance of upstream signaling in Atf3 functions (Figures S7A and S7B; data not shown). TGF-β1 promoted GIC growth in a *Bmi1*-dependent manner but varying Atf3 levels did not alter this response (Figure S7B), although we found that *Bmi1* is important in restraining *Atf3* expression in response to TGF-β1 in human GSCs, and more broadly, to all the TGF-β/BMP ligands (Figures S7C and S7D). Importantly, *Bmi1* depletion relieved *Atf3* repression in GSCs exposed to NPCs-conditioned medium (Figure S7E). Therefore, BMP7 stimulation and ER stress induction using arvanil provide the most biologically relevant signaling context to investigate the tumor suppressive functions of *Atf3*.

As we applied these experimental conditions to *Bmi1*-depleted human mesenchymal GSCs, ATF3 staining increased in both the cytoplasm and nucleus of GBM1 cells (Figures 7A and S7F), and ATF3 ChIP-seq uncovered its binding both at intergenic sites and nearby 2,192 RefSeq genes (Figures 7B, 7C, S7G, and S7H), some of which are highly expressed in human GBM, notably in the mesenchymal subtype along with the TGF-β signaling genes (Figures S7I and S7J).

Strikingly, ATF3 binding did not occur exclusively at ATF/CREB sites as expected, but rather at DNA elements enriched in the AP-1 motif (Figure 7D). ChIP- and DNaseI-qPCR revealed ATF3's preference for DNaseI-accessible c-JUN-primed sites, and Re-ChIP excluded that ATF3 and c-JUN binding was affected by heterogeneity within our cell culture experiments (Figures 7E–7H). Of note, genome-wide colocalization between ATF3 and AP-1(FOS and JUN) is not restricted to glioma cells because we confirmed it in K562 leukemia cells (data not shown). Also, ATF3 binding sites in GBM1 usually bear one or more CAGAC sites (~60%), indicating that BMP7-activated SMADs may be important in target recognition (data not shown). Thus, once derepressed and activated, Atf3 binds to several genomic sites in a signaling- and chromatin structure-oriented manner.

### Atf3 Participates in the Inhibition of Cell-Type-Specific Critical Oncogenic Pathways

To investigate the functional implication of Atf3 activation in GBM1 cells, we performed pathway analysis. The regulatory network governed by ATF3 was enriched for genes downstream of ERK/MAPK signaling, TGF-β, and, strikingly, all the master regulators of the "mesenchymal transcriptional network (MTN)," like *Cebpb*, *Stat3*, *Fosl2*, and *Runx1* (Figures 7C, 8A, and S7G; Table S4; Carro et al., 2010). While the TGF-β/MTN targets are likely to be mesenchymal-GSCs specific, the ERK/MAPK signaling may be more broadly linked to ATF3 activation. In fact mouse GICs and GSCs shared only ~38% and 41% ATF3 targets genes, respectively, with GSCs, while pathway analysis returned similar categories involved in stress-response and MAPK signaling (Figure S8A; data not shown).

To unbiasedly analyze the more critical genes downstream of ATF3, we performed RNA-seq profiling and pathway analysis of GBM1 cells treated with BMP7/arvanil or left untreated. This analysis highlighted the repression of ATF3-ERK/MAPK downstream genes, such as *Pi3kr2* and *Pi3kr3*, and MAP kinase phosphatases (Dusp-1, -4, -9), consistent with the ATF3 transcriptional repressive activity (Figure 8B; Table S4). RT-qPCR confirmed that these genes are significantly downregulated when GBM1 were propagated for 5 days under BMP7/arvanil as opposed to conditions endorsing tumor self-renewal and TGF-β oncogenic activity (EGF/bFGF/TGF-β1; Figure 8C). *Atf3* knockdown in BMP7/arvanil-treated GBM1 cells suggested a prominent role for *Atf3* in the direct regulation of targets involved in the ERK/MAPK pathway (Figure 8D).

In 293T cells treated with an alternative ER stressor (i.e., thapsigargin), we found that neither *Atf3* overexpression nor ER stress induction are sufficient to affect target genes in an *Atf3*-dependent manner and that the TGFβ/BMP-dependent SMAD component appears to be required (i.e., SMAD3 overexpression or TGF-β1 stimulation (Figures S8B and S8C).

Finally, *Atf3* knockdown in T98G glioma cells (more amenable to multiple infection/selection rounds) highlighted its role in supporting arvanil-induced stress response (assessed by stress beacons phospho-p38, -JUN, and -ATF2), while impairment of ERK/MAPK signaling strongly relies on the BMP7 signaling (Figures S8D and S8E). Intriguingly, arvanil induced a feed-forward loop toward *Bmi1* expression, in vitro and in vivo (Figures S8F–S8H; data not shown), supporting our conclusion that *Bmi1* lies at the heart of GSC self-renewal by orchestrating the cellular response to opposing signaling: cooperating with TGF-β-induced self-renewal and opposing the cytostatic function of BMP and ER stress-response pathways, at least in part via repression of *Atf3* (Figure 8E).

## DISCUSSION

*Bmi1* functions are important for normal and tumor development, as we previously demonstrated in neurogenesis and

(D) Box plot illustrating the dropout of ten hairpins targeting EGFR in four GFPi tumors, and four in vitro propagated GICs, as compared to plasmid library and T0 GICs reads. One-way ANOVA, $p < 0.0001$.

(E) Venn diagram depicted the tumor-enriched hairpin overlap between two independent in vivo experiments. One hundred six of 759 CBTG library hairpins were enriched in more than three animals per experiment (Exp1 = 9, Exp2 = 11; $p < 0.0001$, hypergeometric distribution).

(F) Heatmap correlation of each shRNA-seq profiles to each other. Rows and columns (normalized reads) are sorted based on Spearman's rank-order. Yellow and red represent high and low correlations, respectively. Tumor-promoting shRNA were selected using criteria as indicated.

G) RT-qPCR analysis of the human glioma cell line T98G treated for 5 days with either 10 μM 5-azacytidine (5-AzaC) ± dox or vehicle alone. Il5ra is not expressed. Statistics used two-way ANOVA. Note the cooperation between inhibitors.

Error bars = ± SD. See also Figure S4 and Table S3.

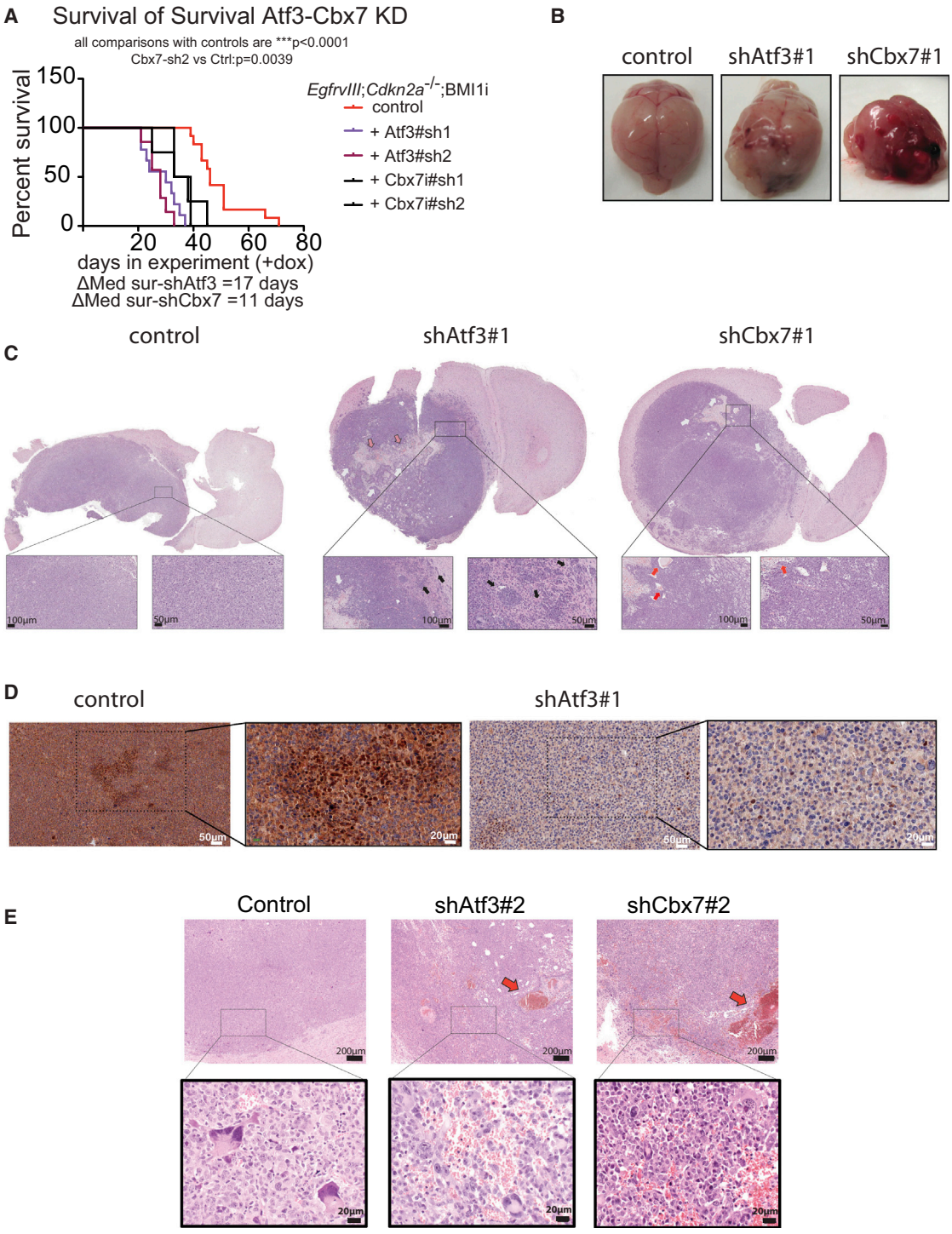


**Figure 5. Suppression of *Atf3* and *Cbx7* in *Bmi1*-Depleted Glioma-Initiating Cells Accelerates Tumorigenesis and Impairs Animal Survival**

(A) GICs co-expressing dox-responsive shBMI1 and two hairpins targeting *Atf3* or *Cbx7* were intracranially injected into recipient mice. Animals were sacrificed on development of neurological signs. Statistics used log-rank (Mantel-Cox) test.

(B) Representative images of tumor-bearing brains.

(C) Representative hematoxylin and eosin (H&E) staining. White, black, red, and pink arrows denote multifocal necrosis, invasive margins, tumor angiogenesis, and fibrovascular stroma, respectively.

(D) IHC staining for tumors from (C).

(E) Representative photomicrographs. Note the hemorrhages (arrows) in *Atf3*- and *Cbx7*-depleted tumors.

See also Figure S5.

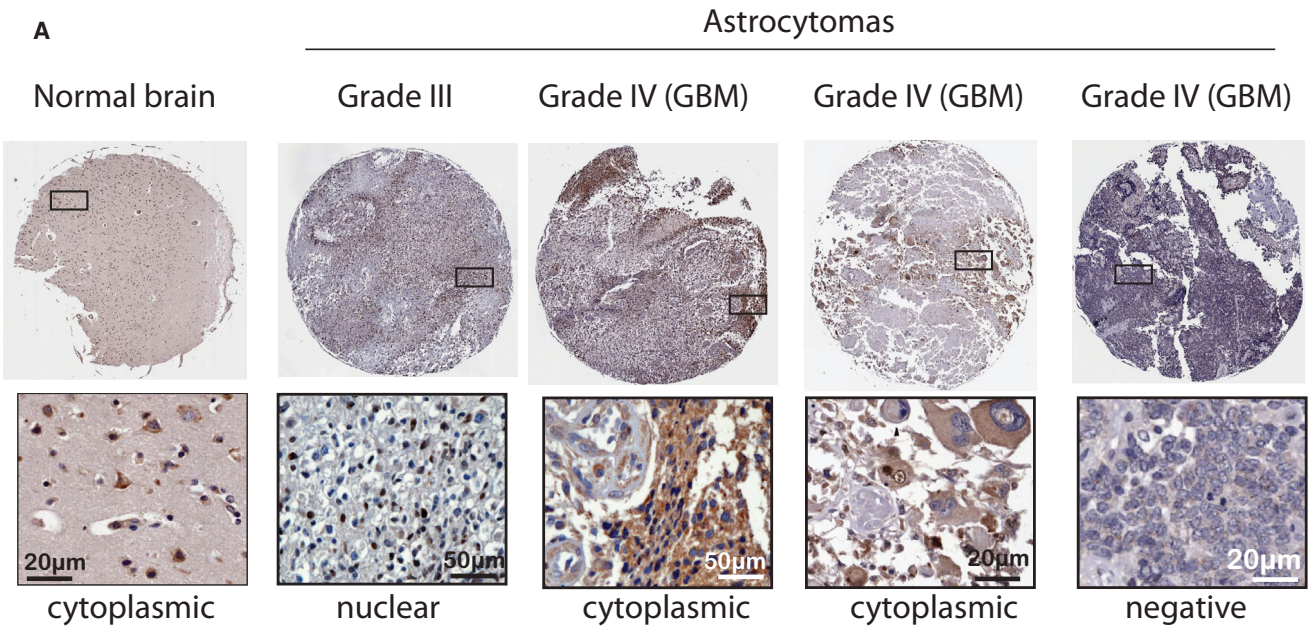


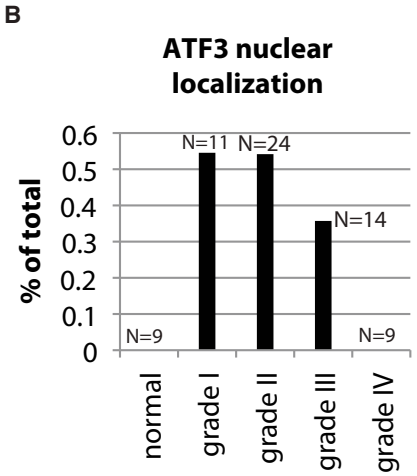


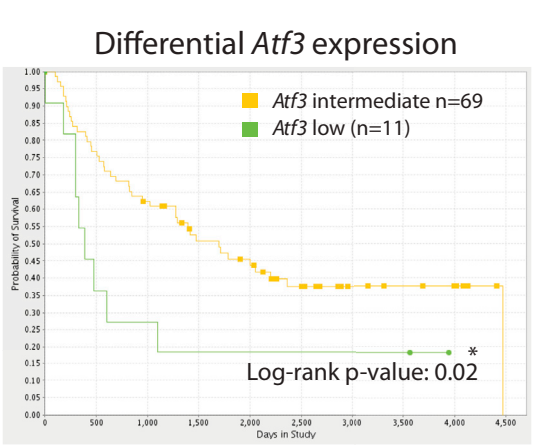


**Figure 6. Low *Atf3* Expression Correlates with Poor Survival in Patients with Astrocytoma**

(A) Representative images for a tissue array bearing 63 tumors and eight normal brain sections stained with anti-ATF3 antibody. Scale bar is indicated. Representative H&E staining at http://www.biomax.us/tissue-arrays/Brain/BS17017.

(B) Quantification of biopsies with nuclear ATF3 in relation to tumor grading.

(C) From NIH Rembrandt database, significant correlation between *Atf3* gene expression and overall survival was found in biopsy specimens from patients with astrocytoma (tumor-grade compatible with ATF3 nuclear expression). Age correction was not necessary because patients with low expression were younger than patients with intermediate expression.

See also Figure S6.

gliomagenesis (Bruggeman et al., 2005, 2007). In multipotent cells, *Bmi1* promotes long-term survival through the repression of the Cdkn2a locus and it also prevents unscheduled differentiation or changes in cell adhesion properties (Pietersen et al., 2008; Bruggeman et al., 2009). To identify critical downstream BMI1 targets and signaling pathways in an unbiased manner, we combined comprehensive BMI1 target identification (ChIP-seq) on mouse and human NPCs, GICs, and GCs with dedicated in vivo shRNAi screening. This study uncovered an important role for *Bmi1* in neural progenitor and glioma cells via the transcriptional repression of genes involved in the cellular response to TGF-β/BMP and ER stress-response signaling pathways. Mechanistically, the prominent role for BMP signaling in neural tissue homeostasis and its functional connection with the BMI1 pathway now support a model in which BMI1/PcG are critically involved in the fine-tuning of cellular responses to the local tumor microenvironment.

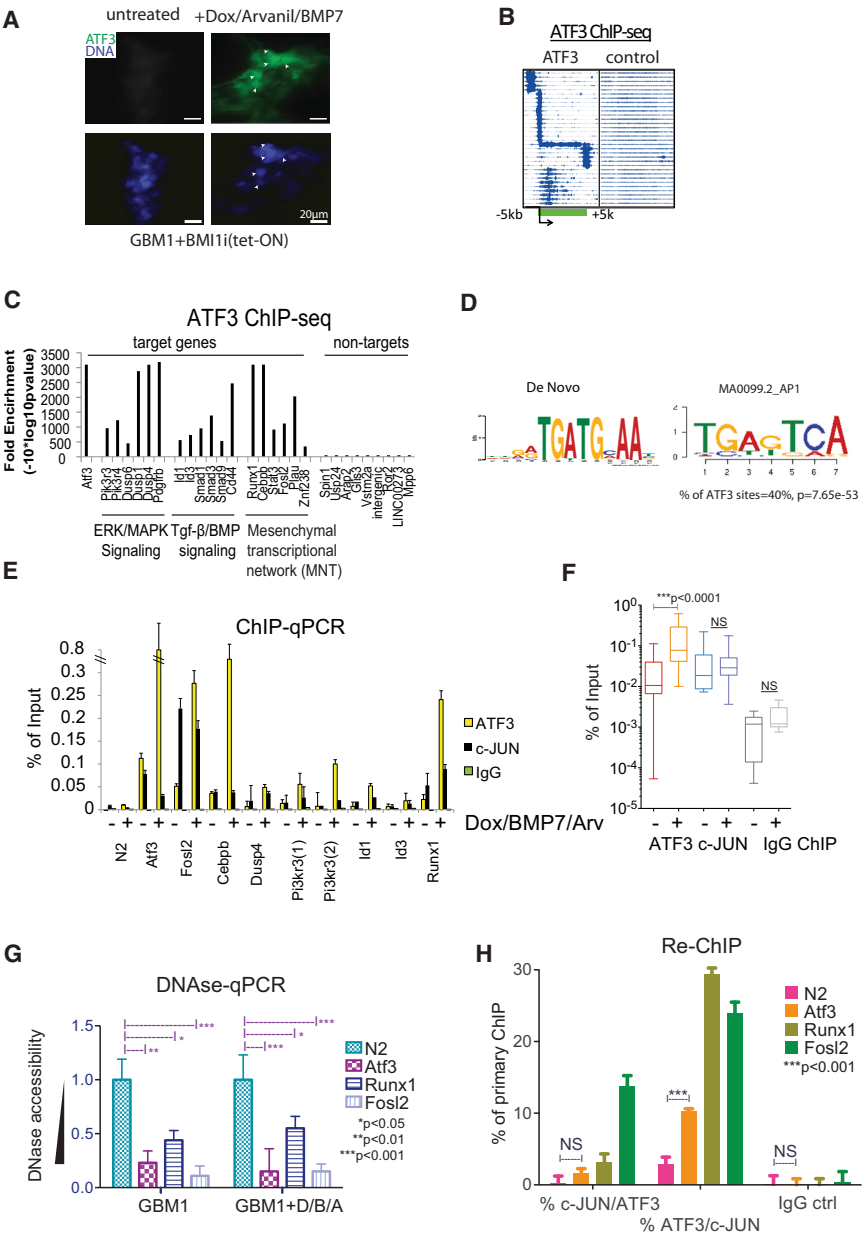


**Figure 7. ATF3 Binding to DNaseI-Accessible Chromatin Preloaded with AP1**

(A) IF for ATF3 in *Bmi1*-depleted GBM1 cells grown under conditions mimicking the antitumorigenic response of endogenous NPCs. Cells were infected with a dox-responsive shBMI1i, treated for 48 hr with doxycycline, 24 hr with ER stressor arvanil, and 3 hr with BMP7.

(B) Horizontal lines represent ATF3 target genes in GBM1 cells propagated as in (A) and dark blue high reads count. Input DNA is shown as control.

(C) Selection of ATF3 target genes from (B).

(D) ATF3 binds to AP1 motifs. De novo and TFBS motif search are shown.

(E) ChIP-qPCR for the indicated genes and antibodies, in dox/BMP7/arvanil-treated GBM1 and untreated cells.

(F) Box plot of data in (E) denotes ATF3 binding to AP1 sites upon induction (unpaired Student's t test).

(G) GBM1 cell nuclei were digested with DNaseI or left untreated and the indicated genomic regions amplified by PCR (amplification inversely correlates with accessibility). Note the higher and stable accessibility of ATF3 binding sites as compared to DnaseI-resistant N2 locus (n = 2; two-way ANOVA).

(H) Re-ChIP-qPCR for ATF3 → c-JUN (left), c-JUN → ATF3 (middle) and IgG → IgG (right) immunoprecipitation experiments. N2 provides background enrichment for each Re-ChIP (n = 2; two-way ANOVA).

Error bars = ± SD. See also Figure S7 and Table S4.

The role of the context—namely the cell-type-specific oncogenetic lesions and the extracellular signaling—seems to be a primary determinant for the function of the genes identified in this screening. For instance, *Cbx7* is capable of promoting or suppressing malignant phenotype conversions, and here we report it to restrain gliomagenesis (Scott et al., 2007; Forzati et al., 2012). Likewise, *Atf3* has been previously proposed to oppose tumorigenesis in colon and prostate cancer models (Huang et al., 2008; Taketani et al., 2011). However, while our data excluded *Atf3* to provide growth advantage under our experimental conditions, it remains possible that oncogenic *Atf3* functions may be elicited due to alternative signaling cascades, differences in cell of origin or cooperating oncogenic lesions, such as WNT signaling or *H-ras*$^{V12}$ as shown in other studies (Wu et al., 2010; Yan et al., 2011).

Because *Atf3* is activated by both developmental and stress pathways, our model proposes a dual action for *Bmi1* in desensitizing the *Atf3* promoter to TGF-β/BMP pathways and to ER stress signaling, possibly by dampening the extent and the duration of *Atf3* induction. The biological relevance for the TGF-β/BMP-*Atf3*-*Bmi1* axis in glioma is highlighted by the recent discovery that endogenous NPCs exert a tumor suppressive function through the release of ER stressors and BMP7 (Chirasani et al., 2010; Stock et al., 2012). The link between PcG and ER stress-regulated *Atf3* may be well conserved because *Atf3* is overexpressed in *Ring1b* mutant zebrafish treated with thapsigargin, a potent inducer of ER stress-dependent apoptosis (unpublished data).

Mechanistically, *Atf3* has been previously involved in *Id1* repression in the context of cell cycle inhibition by TGF-β in non-transformed cells (Kang et al., 2003). *Atf3* derepression also correlated with *Id1* inhibition in glioma cells, but only under a different signaling cascade (tumor necrosis factor-α, not TGF-β; Anido et al., 2010). However, our data suggest that the *Atf3*-dependent transcriptional suppression of *Id1* may not play a pivotal role restraining gliomagenesis, though *Id1* is a direct ATF3 target in GSCs. This may be due to the BMP signaling

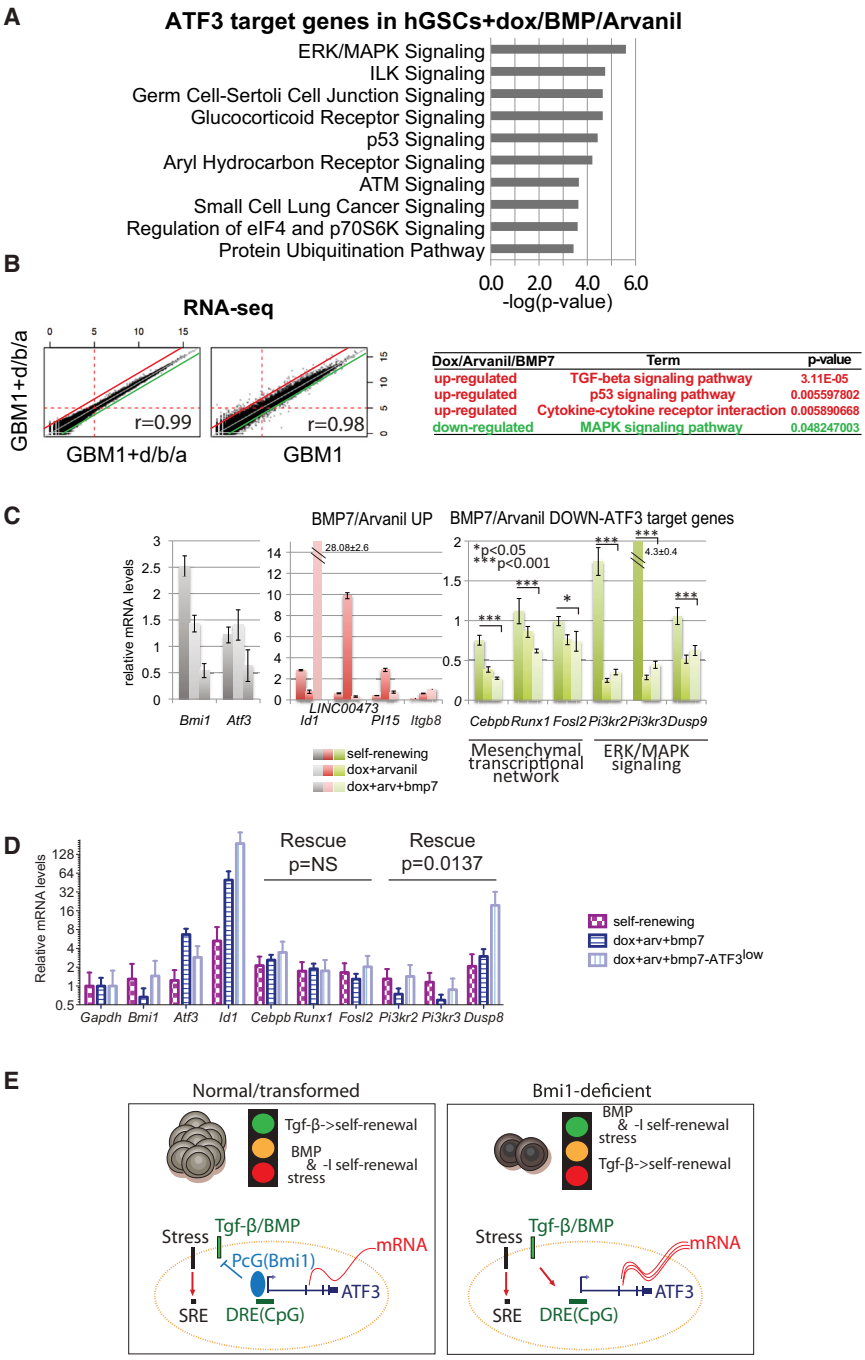


**Figure 8. Significance of ATF3 Functional Activation**

(A) Functional annotation of ATF3 target genes.

(B) RNA-seq for dox/BMP7/arvanil-treated GBM1 cells. Functional annotation of up- and down-regulated genes is shown in red and green, respectively.

(C) RT-qPCR for genes identified in (B) in GBM1 cells propagated under conditions promoting (EGF, bFGF, and TGF-β1) or suppressing self-renewal (doxycycline, arvanil, BMP7). Selected statistical comparisons are show (two-way ANOVA, $p < 0.0001$). Note that BMP7 and arvanil abrogate TGF-β1 induction of ERK/MAPK and MTN ATF3 target genes in *Bmi1*-depleted cells.

(D) RT-qPCR for genes in (C) in GBM1 cells ± shATF3. BMP7/Arvanil treatment occurred 3 hr before lysis. Two-way ANOVA indicates that ERK/MAPK genes are rescued by lower *Atf3* induction.

(E) A model for *Bmi1* integration of opposing signaling in NSCs/GSCs. Suppression of *Atf3* enables oncogenic TGF-β and abrogates BMP cytostatic activity, and occurs through the canonical PcG-mediated transcriptional repression at developmental responsive elements (DRE). The ER stress pathway can still activate *Atf3* transcription, likely through regulatory stress-responsive elements or chromatin regulation, and PcG would restrict the extent and the duration of this pathway.

Error bars = ± SD. See also Figure S8.

promoting alternative uses for *Id1* or to ID1 function itself being dependent on the context in gliomagenesis as previously shown (Anido et al., 2010; Barrett et al., 2012). Intriguingly, one surprising aspect of this study is our observation that *Atf3* activity may be modulated, if not predetermined, by a combination of upstream signaling and local cell-type-specific chromatin structure, notably via "pioneer" transcription factors such as AP1. Indeed, the SMAD(s)-, AP1-, and open-chromatin-aided target gene selection is reminiscent of glucocorticoid receptor binding (Biddie et al., 2011) and suggest a reassessment of the over-simplified model that ATF/CREB DNA binding sites drive ATF3 target selection (Thompson et al., 2009). Because AP1 binding and open chromatin are cell-type-specifically distributed but generally available to all cells, this mechanism provides a molecular basis to investigate GBM-subtype-independent therapeutic strategies aiming at ATF3 functional activation.

Human high-grade gliomas display a remarkable intertumor and intratumor variability, which poses several challenges to effective treatment. Key driving and mutually exclusive oncogenic mutations such as PDGFR (proneural), EGFR (classical), and NF1 (mesenchymal) may in part be responsible for GBM heterogeneity. However, we showed evidence for the *Bmi1-Atf3* axis to widely operate in all subtypes, notably in glioma stem cells. Multiagent therapies exploiting *Atf3* tumor suppressive function should aim at overcoming its cytoplasmic sequestration because we showed that the ER stressor arvanil is not sufficient in achieving full nuclear function of ATF3 despite reducing tumor proliferation and extending animal survival. To this end, it remains to be precisely established whether nuclear ATF3 is driven by phospo-SMAD(s) or by down-modulation of ERK1/2 phosphorylation (Kang et al., 2003; Inoue et al., 2004). Because BMP agonists are not

currently available for therapy, it is tempting to speculate that ERK inhibitors may act as a surrogate to reinforce ATF3 activation. Importantly, our study suggests that BMI1 may simultaneously suppress several genes that could have tumor-suppressive function in glioma. As an epigenetic repressor, BMI1 activity is potentially reversible in vivo. Most likely, dual action cytotoxic/differentiation therapies may effectively impair gliomagenesis, given that most of the tumor-promoting shRNAs/BMI1 target genes are expressed in differentiated neural cell types.

The ChIP-seq/in vivo RNAi screen approach reported here could be used to systematically test otherwise elusive biomarkers and therapeutic targets for cancers. The use of inducible RNAi should be considered to avoid affecting tumor initiation when testing nonsilent genes or to enable cooperative testing of drugs and RNAi. Also, current next-generation RNAi technologies may further limit the contribution of passenger shRNAs or hairpins with inefficient knockdown (Fellmann et al., 2011).

In summary, our study integrates a well-characterized mouse model for glioma, genome-wide BMI1 binding profiles, and an in vivo forward genetic screen with the ultimate goal of identifying clinically relevant cancer genes, with possible translational implications.

## EXPERIMENTAL PROCEDURES

Primary cell derivation and propagation, ChIP and immunohistochemistry protocols were previously described (Bruggeman et al., 2007; Gargiulo et al., 2009), Detailed protocols, plasmids, and antibodies are reported in the Supplemental Experimental Procedures. Patient-derived line samples were not generated for this study (referenced elsewhere). All animal experiments were conducted in compliance with the European Union guidelines for the use and care of laboratory animals and were reviewed and approved by the animal ethics committee (DEC) of the Netherland Cancer Institute.

### RNAi Screen

GICs cells were infected with a dox-inducible shRNA against GFP or BMI1, FACS purified by GFP expression, and $4 \times 10^6$ cells were infected with a shRNA library targeting a 159 gene set (789 hairpins), pooled from individual clones from the TRC library (Open Biosystems), and packaged in a high titer lentiviral prep (>$2 \times 10^5$ IFU/ml). Twenty-four hours after infection, GICs cells were puromycin selected. Next, $1 \times 10^5$ GICs cells per mouse, representing >125-fold enrichment over the library, were injected intracranially into NOD/SCID mice. For the number of actual integrations, $4.5 \times 10^5$ noninjected remaining cells were used as a calibrator. Disease progression was monitored by symptoms ~5–7 weeks after injection, and tumor tissues were surgically resected. Hematoxylin and eosin staining on one representative tumor confirmed high-grade glioma formation. shRNAs were amplified from genomic DNA using primers that include adaptors for Illumina Hiseq sequencing. After PCR amplification of hairpins, sequencing was used to identify constituent shRNAs in each sample. The sequence reads were aligned to a list of all shRNAs of the TRC library. Fold change in hairpin representation after proliferation in vitro or in vivo was determined by comparing shRNA representation in each sample to that in a control cell population remaining after cell intracranial injection.

## ACCESSION NUMBER

The GEO accession number for the raw data for ChIP/RNA-seq data reported in this paper is GSE33912.

## SUPPLEMENTAL INFORMATION

Supplemental Information includes eight figures, four tables, and Supplemental Experimental Procedures and can be found with this article online at http://dx.doi.org/10.1016/j.ccr.2013.03.030.

## ACKNOWLEDGMENTS

We thank E. Tanger, E. Ozay, D. Koldere, K. El Messaoudi, and F.Gargiulo for technical assistance; P. Possik and K. Greig for advice on RNAi screen; J. Song for pathology assessment; Y.v.d. Velden and AP Haramis for unenclosed experiments; Peter Dirks, Steve Pollard, and Rainer Glass for sharing unpublished results and reagents; and NKI Microarray, Microscopy, Screening, FACS, and Animal Facilities for assistance with experiments. We are indebted to W. Aktar, A. Alendar, A. Kraft, E. Guccione, and A. Sparmann for critically reading the manuscript. This study was supported by the European Commission projects FCMOG to G.G. and ESTOOLs, the Netherlands Genomics Initiative, and the BSIK 03038 program grant "stem cells in Development and Disease" to M.v.L.

Received: September 6, 2012
Revised: January 10, 2013
Accepted: March 29, 2013
Published: May 13, 2013

## REFERENCES

Abdouh, M., Facchino, S., Chatoo, W., Balasingam, V., Ferreira, J., and Bernier, G. (2009). BMI1 sustains human glioblastoma multiforme stem cell renewal. J. Neurosci. *29*, 8884–8896.

Anido, J., Sáez-Borderías, A., Gonzàlez-Juncà, A., Rodón, L., Folch, G., Carmona, M.A., Prieto-Sánchez, R.M., Barba, I., Martínez-Sáez, E., Prudkin, L., et al. (2010). TGF-β receptor inhibitors target the CD44(high)/Id1(high) glioma-initiating cell population in human glioblastoma. Cancer Cell *18*, 655–668.

Bachoo, R.M., Maher, E.A., Ligon, K.L., Sharpless, N.E., Chan, S.S., You, M.J., Tang, Y., DeFrances, J., Stover, E., Weissleder, R., et al. (2002). Epidermal growth factor receptor and Ink4a/Arf: convergent mechanisms governing terminal differentiation and transformation along the neural stem cell to astrocyte axis. Cancer Cell *1*, 269–277.

Barrett, L.E., Granot, Z., Coker, C., Iavarone, A., Hambardzumyan, D., Holland, E.C., Nam, H.-S., and Benezra, R. (2012). Self-renewal does not predict tumor growth potential in mouse models of high-grade glioma. Cancer Cell *21*, 11–24.

Biddie, S.C., John, S., Sabo, P.J., Thurman, R.E., Johnson, T.A., Schiltz, R.L., Miranda, T.B., Sung, M.-H., Trump, S., Lightman, S.L., et al. (2011). Transcription factor AP1 potentiates chromatin accessibility and glucocorticoid receptor binding. Mol. Cell *43*, 145–155.

Bric, A., Miething, C., Bialucha, C.U., Scuoppo, C., Zender, L., Krasnitz, A., Xuan, Z., Zuber, J., Wigler, M., Hicks, J., et al. (2009). Functional identification of tumor-suppressor genes through an in vivo RNA interference screen in a mouse lymphoma model. Cancer Cell *16*, 324–335.

Bruggeman, S.W.M., Valk-Lingbeek, M.E., van der Stoop, P.P.M., Jacobs, J.J.L., Kieboom, K., Tanger, E., Hulsman, D., Leung, C., Arsenijevic, Y., Marino, S., and van Lohuizen, M. (2005). Ink4a and Arf differentially affect cell proliferation and neural stem cell self-renewal in Bmi1-deficient mice. Genes Dev. *19*, 1438–1443.

Bruggeman, S.W.M., Hulsman, D., Tanger, E., Buckle, T., Blom, M., Zevenhoven, J., van Tellingen, O., and van Lohuizen, M. (2007). Bmi1 controls tumor development in an Ink4a/Arf-independent manner in a mouse model for glioma. Cancer Cell *12*, 328–341.

Bruggeman, S.W.M., Hulsman, D., and van Lohuizen, M. (2009). Bmi1 deficient neural stem cells have increased integrin dependent adhesion to self-secreted matrix. Biochim. Biophys. Acta *1790*, 351–360.

Büschges, R., Weber, R.G., Actor, B., Lichter, P., Collins, V.P., and Reifenberger, G. (1999). Amplification and expression of cyclin D genes (CCND1, CCND2 and CCND3) in human malignant gliomas. Brain Pathol. *9*, 435–442.

Cahoy, J.D., Emery, B., Kaushal, A., Foo, L.C., Zamanian, J.L., Christopherson, K.S., Xing, Y., Lubischer, J.L., Krieg, P.A., Krupenko, S.A., et al. (2008). A transcriptome database for astrocytes, neurons, and oligodendrocytes: a new resource for understanding brain development and function. J. Neurosci. *28*, 264–278.

Carro, M.S., Lim, W.K., Alvarez, M.J., Bollo, R.J., Zhao, X., Snyder, E.Y., Sulman, E.P., Anne, S.L., Doetsch, F., Colman, H., et al. (2010). The transcriptional network for mesenchymal transformation of brain tumours. Nature *463*, 318–325.

Chirasani, S.R., Sternjak, A., Wend, P., Momma, S., Campos, B., Herrmann, I.M., Graf, D., Mitsiadis, T., Herold-Mende, C., Besser, D., et al. (2010). Bone morphogenetic protein-7 release from endogenous neural precursor cells suppresses the tumourigenicity of stem-like glioblastoma cells. Brain *133*, 1961–1972.

Facchino, S., Abdouh, M., Chatoo, W., and Bernier, G. (2010). BMI1 confers radioresistance to normal and cancerous neural stem cells through recruitment of the DNA damage response machinery. J. Neurosci. *30*, 10096–10111.

Fellmann, C., Zuber, J., McJunkin, K., Chang, K., Malone, C.D., Dickins, R.A., Xu, Q., Hengartner, M.O., Elledge, S.J., Hannon, G.J., and Lowe, S.W. (2011). Functional identification of optimized RNAi triggers using a massively parallel sensor assay. Mol. Cell *41*, 733–746.

Forzati, F., Federico, A., Pallante, P., Abbate, A., Esposito, F., Malapelle, U., Sepe, R., Palma, G., Troncone, G., Scarfò, M., et al. (2012). CBX7 is a tumor suppressor in mice and humans. J. Clin. Invest. *122*, 612–623.

Gargiulo, G., Levy, S., Bucci, G., Romanenghi, M., Fornasari, L., Beeson, K.Y., Goldberg, S.M., Cesaroni, M., Ballarini, M., Santoro, F., et al. (2009). NA-Seq: a discovery tool for the analysis of chromatin structure and dynamics during differentiation. Dev. Cell *16*, 466–481.

Holland, E.C., Hively, W.P., DePinho, R.A., and Varmus, H.E. (1998). A constitutively active epidermal growth factor receptor cooperates with disruption of G1 cell-cycle arrest pathways to induce glioma-like lesions in mice. Genes Dev. *12*, 3675–3685.

Huang, X., Li, X., and Guo, B. (2008). KLF6 induces apoptosis in prostate cancer cells through up-regulation of ATF3. J. Biol. Chem. *283*, 29795–29801.

Inoue, K., Zama, T., Kamimoto, T., Aoki, R., Ikeda, Y., Kimura, H., and Hagiwara, M. (2004). TNFalpha-induced ATF3 expression is bidirectionally regulated by the JNK and ERK pathways in vascular endothelial cells. Genes Cells *9*, 59–70.

Kang, Y., Chen, C.-R., and Massagué, J. (2003). A self-enabling TGFbeta response coupled to stress signaling: Smad engages stress response factor ATF3 for Id1 repression in epithelial cells. Mol. Cell *11*, 915–926.

Kimmelman, A.C., Qiao, R.F., Narla, G., Banno, A., Lau, N., Bos, P.D., Nuñez Rodriguez, N., Liang, B.C., Guha, A., Martignetti, J.A., et al. (2004). Suppression of glioblastoma tumorigenicity by the Kruppel-like transcription factor KLF6. Oncogene *23*, 5077–5083.

Kioussi, C., Briata, P., Baek, S.H., Rose, D.W., Hamblet, N.S., Herman, T., Ohgi, K.A., Lin, C., Gleiberman, A., Wang, J., et al. (2002). Identification of a Wnt/Dvl/beta-Catenin —> Pitx2 pathway mediating cell-type-specific proliferation during development. Cell *111*, 673–685.

Kriegstein, A., and Alvarez-Buylla, A. (2009). The glial nature of embryonic and adult neural stem cells. Annu. Rev. Neurosci. *32*, 149–184.

Lee, J., Son, M.J., Woolard, K., Donin, N.M., Li, A., Cheng, C.H., Kotliarova, S., Kotliarov, Y., Walling, J., Ahn, S., et al. (2008). Epigenetic-mediated dysfunction of the bone morphogenetic protein pathway inhibits differentiation of glioblastoma-initiating cells. Cancer Cell *13*, 69–80.

Leung, C., Lingbeek, M., Shakhova, O., Liu, J., Tanger, E., Saremaslani, P., Van Lohuizen, M., and Marino, S. (2004). Bmi1 is essential for cerebellar development and is overexpressed in human medulloblastomas. Nature *428*, 337–341.

Lim, D.A., Tramontin, A.D., Trevejo, J.M., Herrera, D.G., García-Verdugo, J.M., and Alvarez-Buylla, A. (2000). Noggin antagonizes BMP signaling to create a niche for adult neurogenesis. Neuron *28*, 713–726.

Meacham, C.E., Ho, E.E., Dubrovsky, E., Gertler, F.B., and Hemann, M.T. (2009). In vivo RNAi screening identifies regulators of actin dynamics as key determinants of lymphoma progression. Nat. Genet. *41*, 1133–1137.

Molofsky, A.V., Pardal, R., Iwashita, T., Park, I.-K., Clarke, M.F., and Morrison, S.J. (2003). Bmi-1 dependence distinguishes neural stem cell self-renewal from progenitor proliferation. Nature *425*, 962–967.

Molofsky, A.V., Slutsky, S.G., Joseph, N.M., He, S., Pardal, R., Krishnamurthy, J., Sharpless, N.E., and Morrison, S.J. (2006). Increasing p16INK4a expression decreases forebrain progenitors and neurogenesis during ageing. Nature *443*, 448–452.

Nam, H.-S., and Benezra, R. (2009). High levels of Id1 expression define B1 type adult neural stem cells. Cell Stem Cell *5*, 515–526.

Ohm, J.E., McGarvey, K.M., Yu, X., Cheng, L., Schuebel, K.E., Cope, L., Mohammad, H.P., Chen, W., Daniel, V.C., Yu, W., et al. (2007). A stem cell-like chromatin pattern may predispose tumor suppressor genes to DNA hypermethylation and heritable silencing. Nat. Genet. *39*, 237–242.

Park, D.M., Sathornsumetee, S., and Rich, J.N. (2010). Medical oncology: treatment and management of malignant gliomas. Nat. Rev. Clin. Oncol. *7*, 75–77.

Pietersen, A.M., Evers, B., Prasad, A.A., Tanger, E., Cornelissen-Steijger, P., Jonkers, J., and van Lohuizen, M. (2008). Bmi1 regulates stem cells and proliferation and differentiation of committed cells in mammary epithelium. Curr. Biol. *18*, 1094–1099.

Pollard, S.M., Yoshikawa, K., Clarke, I.D., Danovi, D., Stricker, S., Russell, R., Bayani, J., Head, R., Lee, M., Bernstein, M., et al. (2009). Glioma stem cell lines expanded in adherent culture have tumor-specific phenotypes and are suitable for chemical and genetic screens. Cell Stem Cell *4*, 568–580.

Schlesinger, Y., Straussman, R., Keshet, I., Farkash, S., Hecht, M., Zimmerman, J., Eden, E., Yakhini, Z., Ben-Shushan, E., Reubinoff, B.E., et al. (2007). Polycomb-mediated methylation on Lys27 of histone H3 pre-marks genes for de novo methylation in cancer. Nat. Genet. *39*, 232–236.

Scott, C.L., Gil, J., Hernando, E., Teruya-Feldstein, J., Narita, M., Martínez, D., Visakorpi, T., Mu, D., Cordon-Cardo, C., Peters, G., et al. (2007). Role of the chromobox protein CBX7 in lymphomagenesis. Proc. Natl. Acad. Sci. USA *104*, 5389–5394.

Seoane, J. (2009). TGFbeta and cancer initiating cells. Cell Cycle *8*, 3787–3788.

Sparmann, A., and van Lohuizen, M. (2006). Polycomb silencers control cell fate, development and cancer. Nat. Rev. Cancer *6*, 846–856.

Stock, K., Kumar, J., Synowitz, M., Petrosino, S., Imperatore, R., Smith, E.S.J., Wend, P., Purfürst, B., Nuber, U.A., Gurok, U., et al. (2012). Neural precursor cells induce cell death of high-grade astrocytomas through stimulation of TRPV1. Nat. Med. Published online July 22, 2012. http://dx.doi.org/10.1038/nm.2827.

Sun, Y., Kong, W., Falk, A., Hu, J., Zhou, L., Pollard, S., and Smith, A. (2009). CD133 (Prominin) negative human neural stem cells are clonogenic and tripotent. PLoS ONE *4*, e5498.

Taketani, K., Kawauchi, J., Tanaka-Okamoto, M., Ishizaki, H., Tanaka, Y., Sakai, T., Miyoshi, J., Maehara, Y., and Kitajima, S. (2011). Key role of ATF3 in p53-dependent DR5 induction upon DNA damage of human colon cancer cells. Oncogene *31*, 2210–2221.

Thompson, M.R., Xu, D., and Williams, B.R.G. (2009). ATF3 transcription factor and its emerging roles in immunity and cancer. J. Mol. Med. *87*, 1053–1060.

van der Lugt, N.M., Domen, J., Linders, K., van Roon, M., Robanus-Maandag, E., te Riele, H., van der Valk, M., Deschamps, J., Sofroniew, M., van Lohuizen, M., et al. (1994). Posterior transformation, neurological abnormalities, and severe hematopoietic defects in mice with a targeted deletion of the bmi-1 proto-oncogene. Genes Dev. *8*, 757–769.

Veeriah, S., Brennan, C., Meng, S., Singh, B., Fagin, J.A., Solit, D.B., Paty, P.B., Rohle, D., Vivanco, I., Chmielecki, J., et al. (2009). The tyrosine phosphatase PTPRD is a tumor suppressor that is frequently inactivated and mutated in glioblastoma and other human cancers. Proc. Natl. Acad. Sci. USA *106*, 9435–9440.

Verhaak, R.G.W., Hoadley, K.A., Purdom, E., Wang, V., Qi, Y., Wilkerson, M.D., Miller, C.R., Ding, L., Golub, T., Mesirov, J.P., et al.; Cancer Genome Atlas Research Network. (2010). Integrated genomic analysis identifies clinically relevant subtypes of glioblastoma characterized by abnormalities in PDGFRA, IDH1, EGFR, and NF1. Cancer Cell *17*, 98–110.

Watabe, T., and Miyazono, K. (2009). Roles of TGF-beta family signaling in stem cell renewal and differentiation. Cell Res. *19*, 103–115.

Widschwendter, M., Fiegl, H., Egle, D., Mueller-Holzner, E., Spizzo, G., Marth, C., Weisenberger, D.J., Campan, M., Young, J., Jacobs, I., and Laird, P.W. (2007). Epigenetic stem cell signature in cancer. Nat. Genet. *39*, 157–158.

Wimmer, K., Zhu Xx, X.-X., Rouillard, J.M., Ambros, P.F., Lamb, B.J., Kuick, R., Eckart, M., Weinhäusl, A., Fonatsch, C., and Hanash, S.M. (2002). Combined restriction landmark genomic scanning and virtual genome scans identify a novel human homeobox gene, ALX3, that is hypermethylated in neuroblastoma. Genes Chromosomes Cancer *33*, 285–294.

Wu, X., Nguyen, B.-C., Dziunycz, P., Chang, S., Brooks, Y., Lefort, K., Hofbauer, G.F.L., and Dotto, G.P. (2010). Opposing roles for calcineurin and ATF3 in squamous skin cancer. Nature *465*, 368–372.

Yan, L., Della Coletta, L., Powell, K.L., Shen, J., Thames, H., Aldaz, C.M., and MacLeod, M.C. (2011). Activation of the canonical Wnt/β-catenin pathway in ATF3-induced mammary tumors. PLoS ONE *6*, e16515.